Supporting Information

Predicting Unprecedented Hot Temperature Extreme Occurrences Up to a Year in Advance

P. De Luca[1], J.C. Acosta Navarro[2], E.M. Fischer[3], and M.G. Donat[1,4]

[1]Barcelona Supercomputing Center (BSC), Barcelona, Spain

[2]European Commission, Joint Research Centre, Ispra, Italy

[3]Institute for Atmospheric and Climate Science, ETH Zurich, Zurich, Switzerland

[4]Institució Catalana de Recerca i Estudis Avançats (ICREA), Barcelona, Spain

Corresponding author: Paolo De Luca, 87paolo11@gmail.com

Supporting Figures

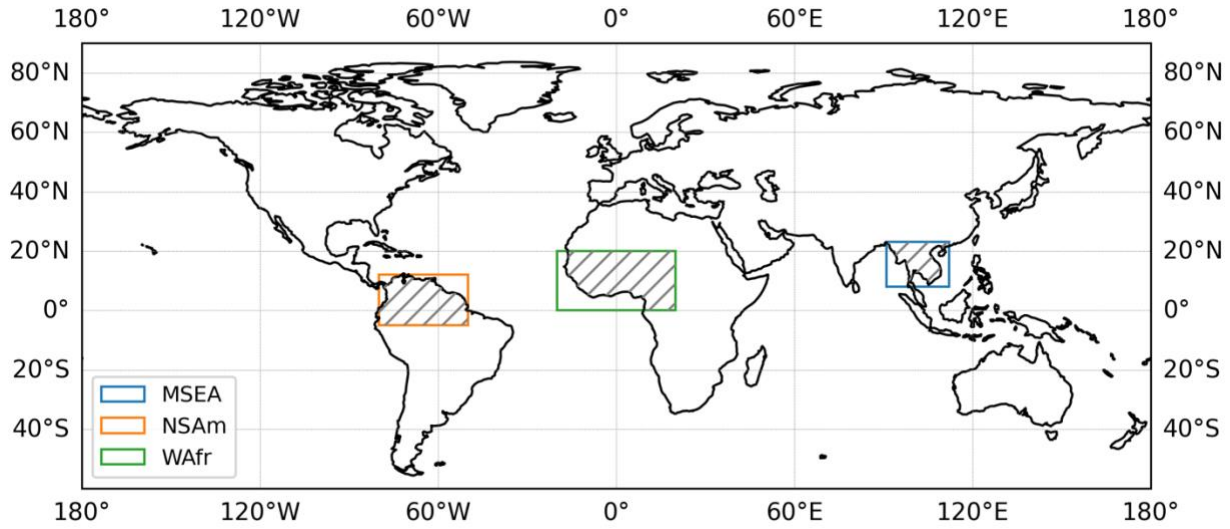


Figure S1. The three regions used for more detailed analysis of UTEx predictability: Mainland Southeast Asia (MSEA, 91°E–112°E, 8°N–23°N) Northern South America (NSAm, 80°W–50°W, 5°S–12°N); and Western Africa (WAfr, 20°W–20°E, 0°N–20°N). Only hatched areas are used, since they represent land grid-points.

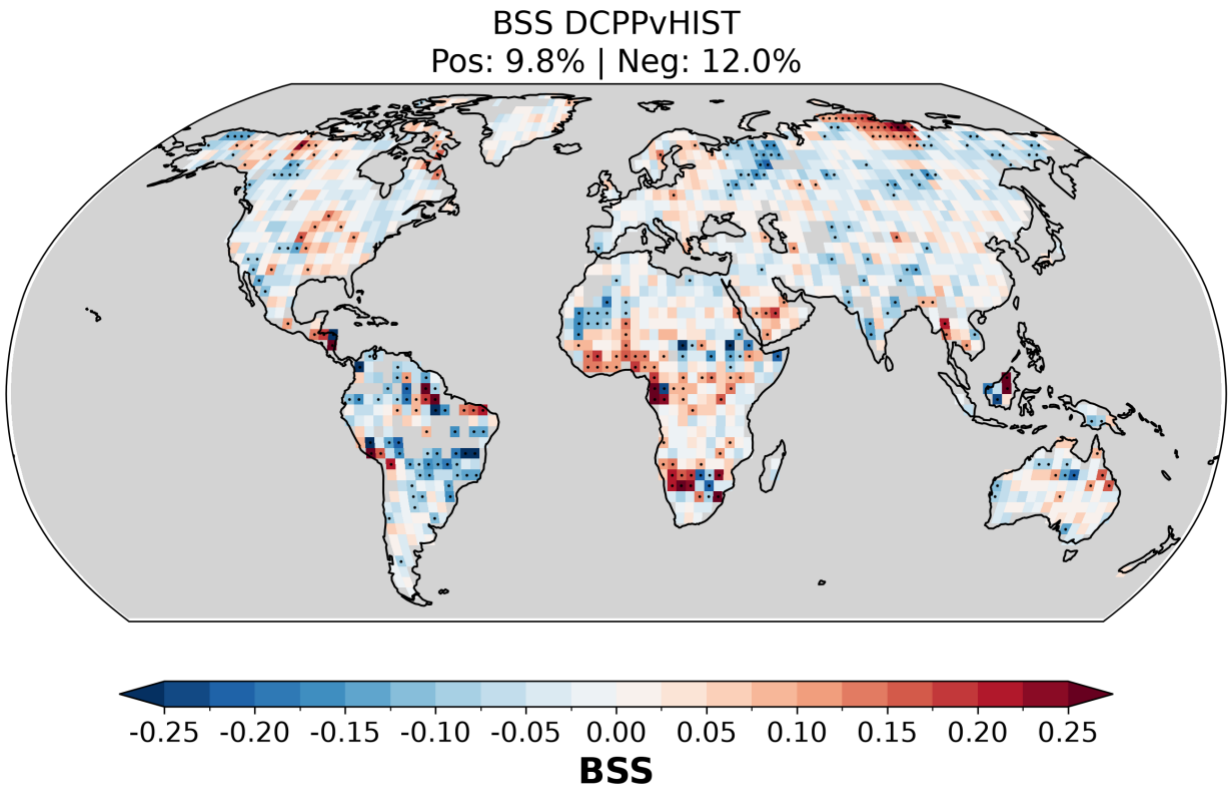


Figure S2. BSS of DCPP using HIST as reference forecast and ObsEns as observational dataset, indicating the added skill of DCPP over HIST for the 1971-2024 period. Pos and Neg indicate the percentage (%) of total global land area (excluded Antarctica) with significant positive and negative skill.

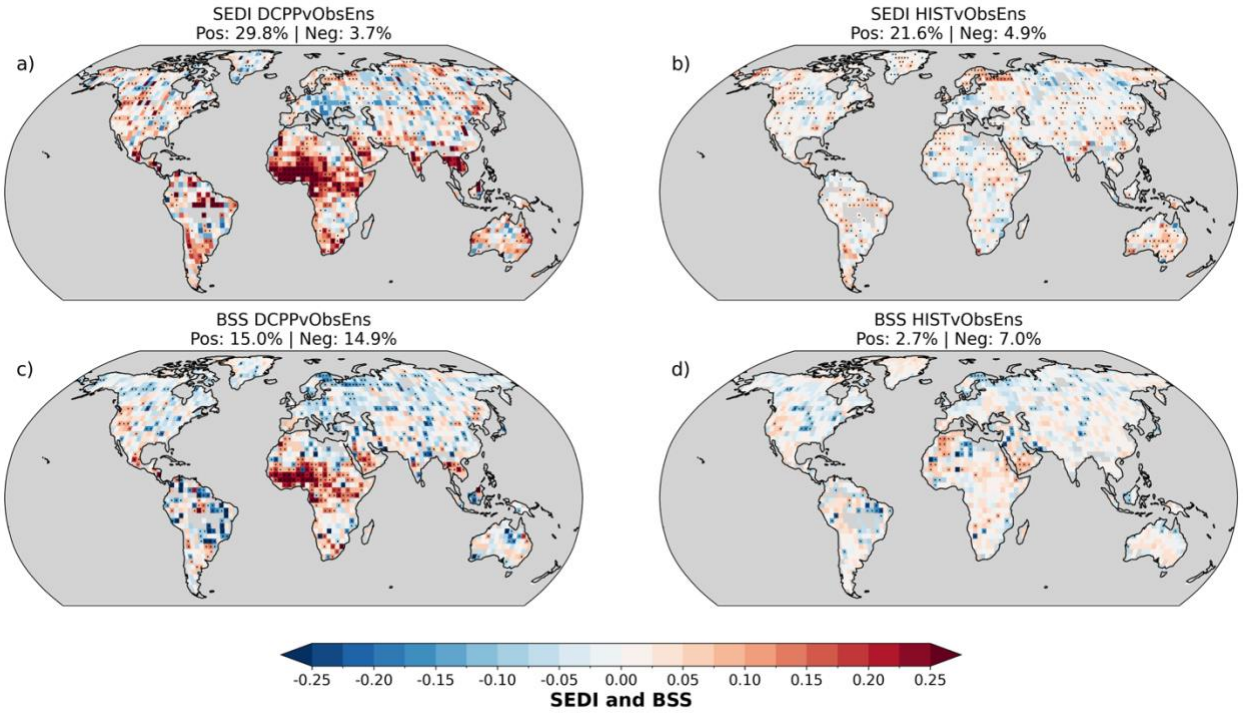


Figure S3. As Figure 1 but for UTEx computed based on absolute temperature values as opposed to anomalies.

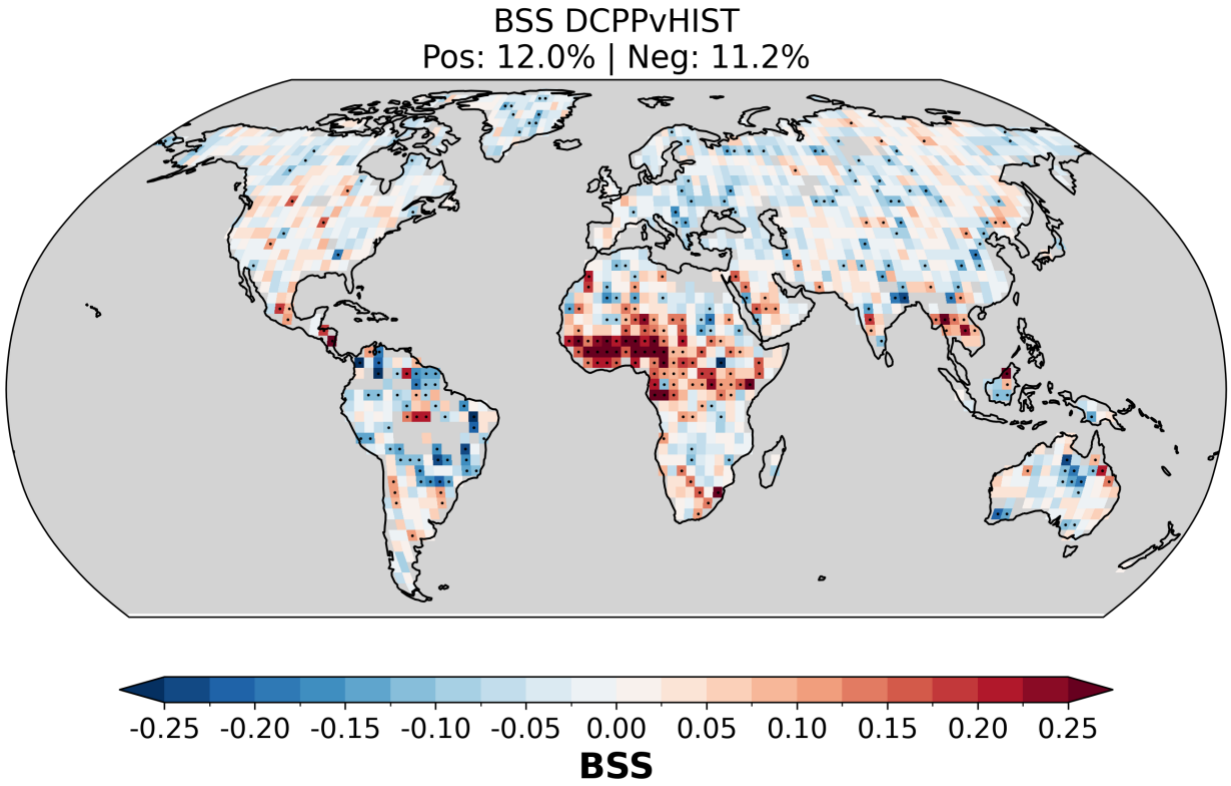


Figure S4. As Figure S2 but for UTEx computed based on absolute temperature values.

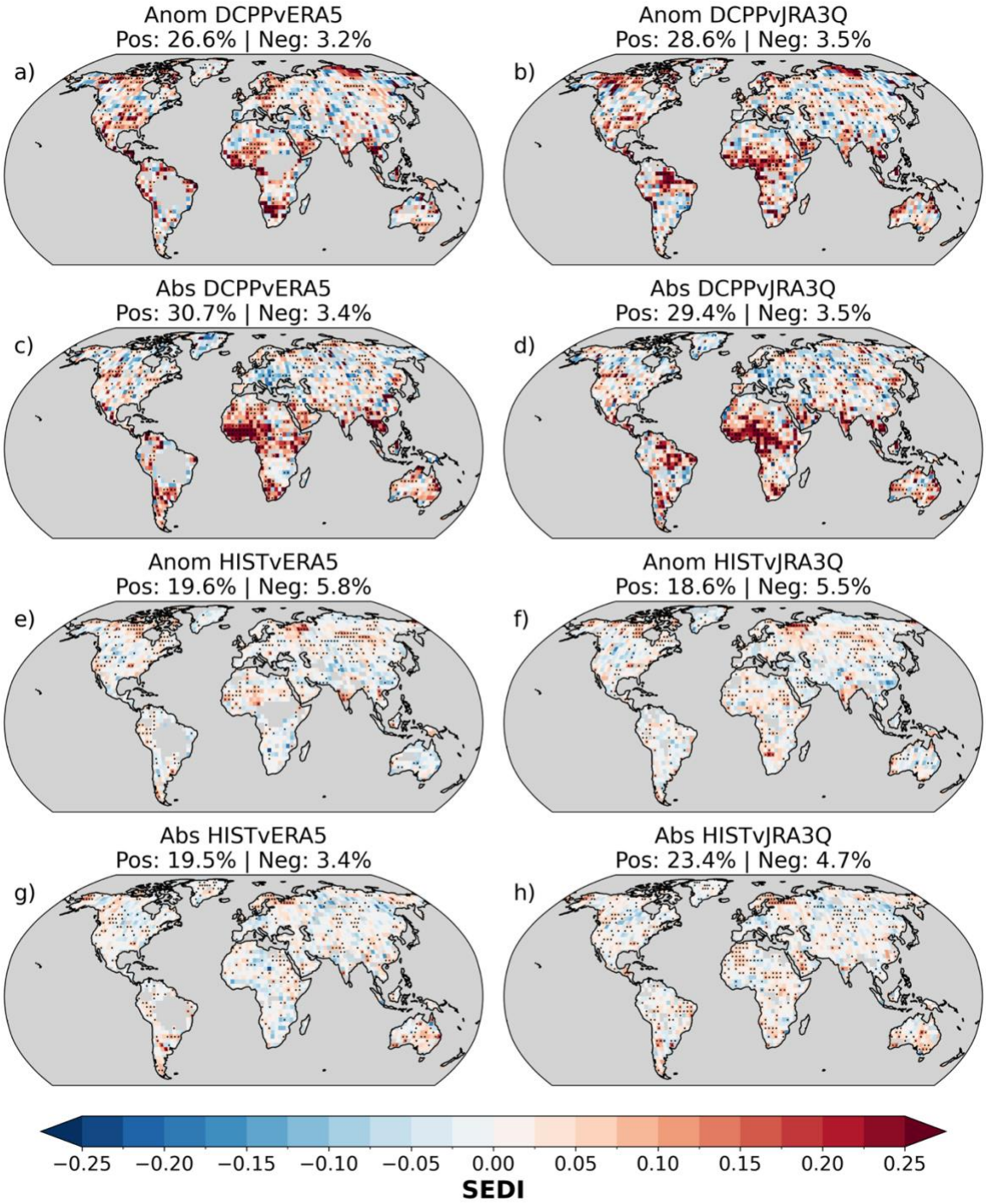


Figure S5. UTEx annual prediction skill for the individual observations-based datasets computed with the SEDI for the 1971-2024 period. (a-f) DCPP skill for anomaly and absolute UTEx; (g-l) HIST skill. Observations-based datasets are: ERA5 and JRA3Q. Stippling indicate grid-points statistically significant (p-value <0.05, two-sided bootstrap, with n=1000 samples). Pos and Neg indicate the percentage (%) of total global land area (excluded Antarctica) with significant positive and negative skill.

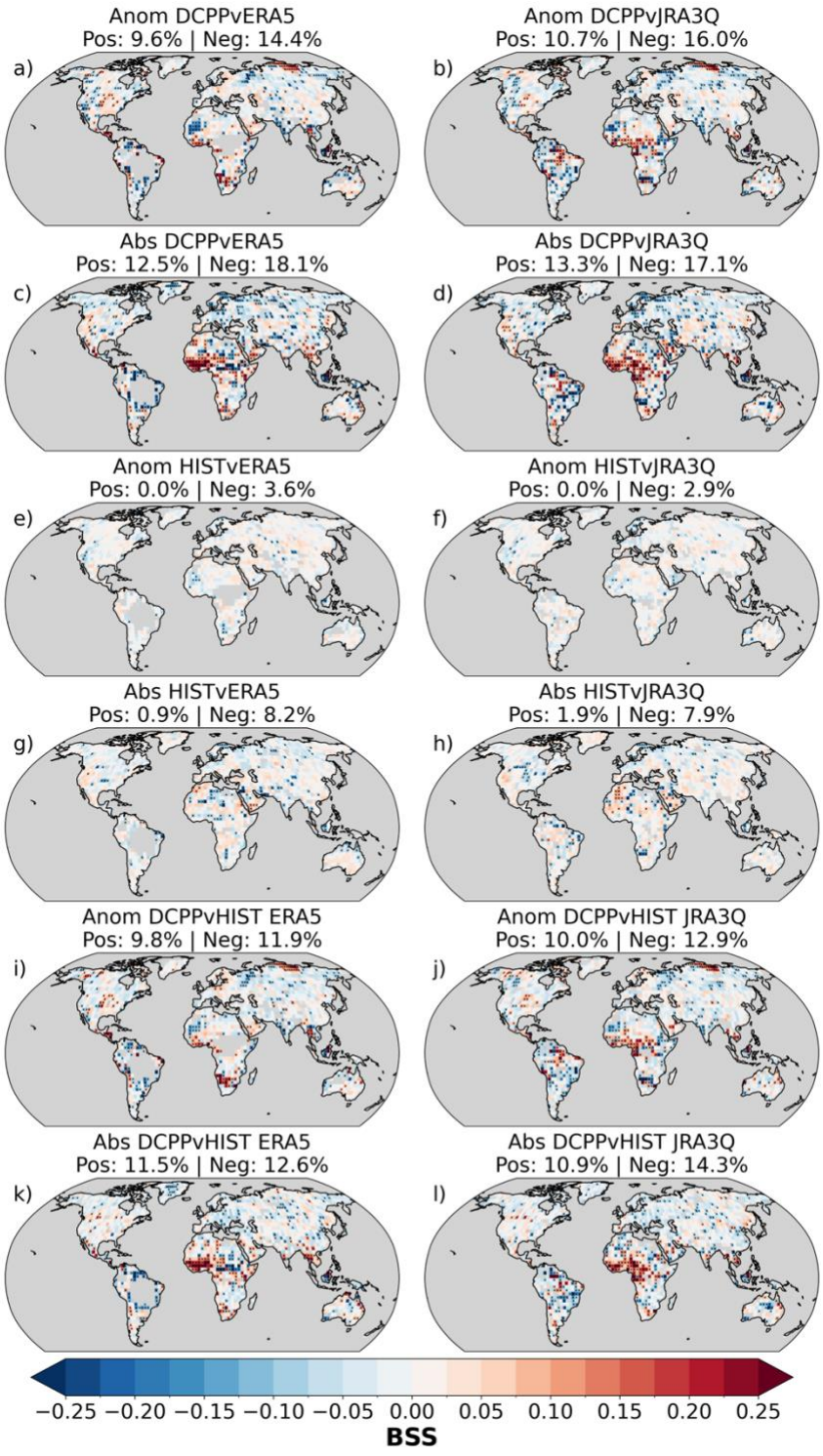


Figure S6. UTEx annual prediction skill for the individual observations-based datasets computed with the BSS for the 1971-2024 period. (a-f) DCPP skill for anomaly and absolute UTEx; (g-l) HIST skill; and (m-r) added skill of DCPP against HIST annual prediction. Observations-based datasets are: ERA5 and JRA3Q. Stippling indicate grid-points statistically significant (p-value <0.05, two-sided bootstrap, with n=1000 samples). Pos and Neg indicate the percentage (%) of total global land area (excluded Antarctica) with significant positive and negative skill.

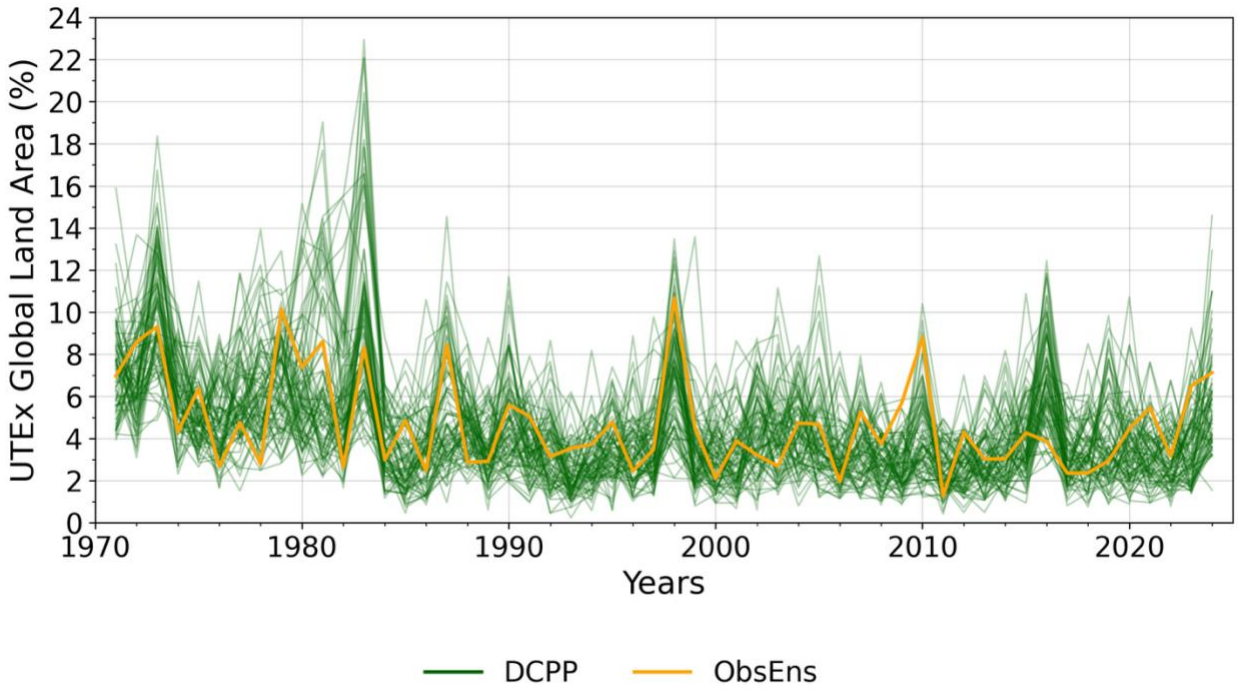


Figure S7. As Figure 2 but for ObsEns and DCPP MME only. For DCPP we show all the 76 individual members.

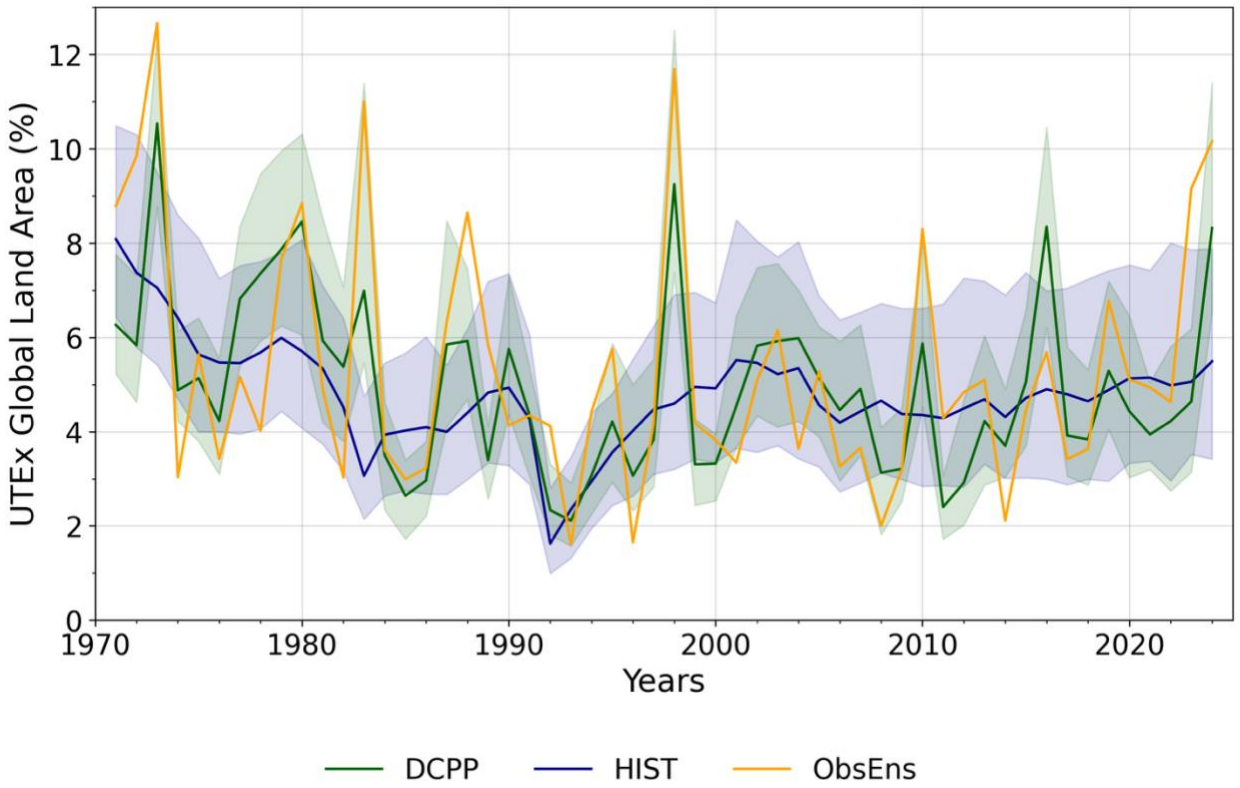


Figure S8. As Figure 2 but for UTEx computed based on absolute temperature values.

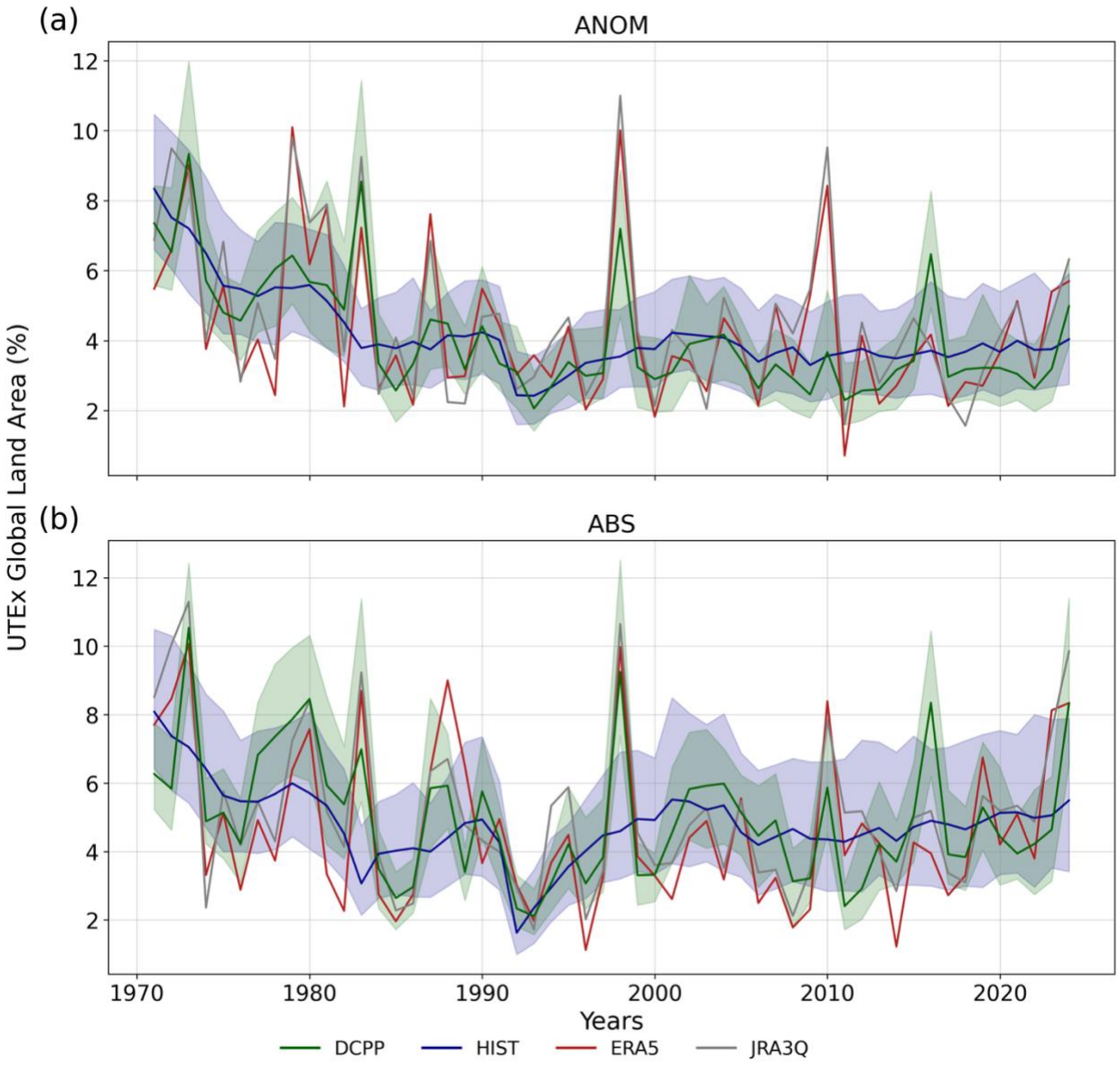


Figure S9. (a) As Figure 2 and (b) as Figure S8 but showing all individual observations-based datasets used as reference instead of ObsEns.

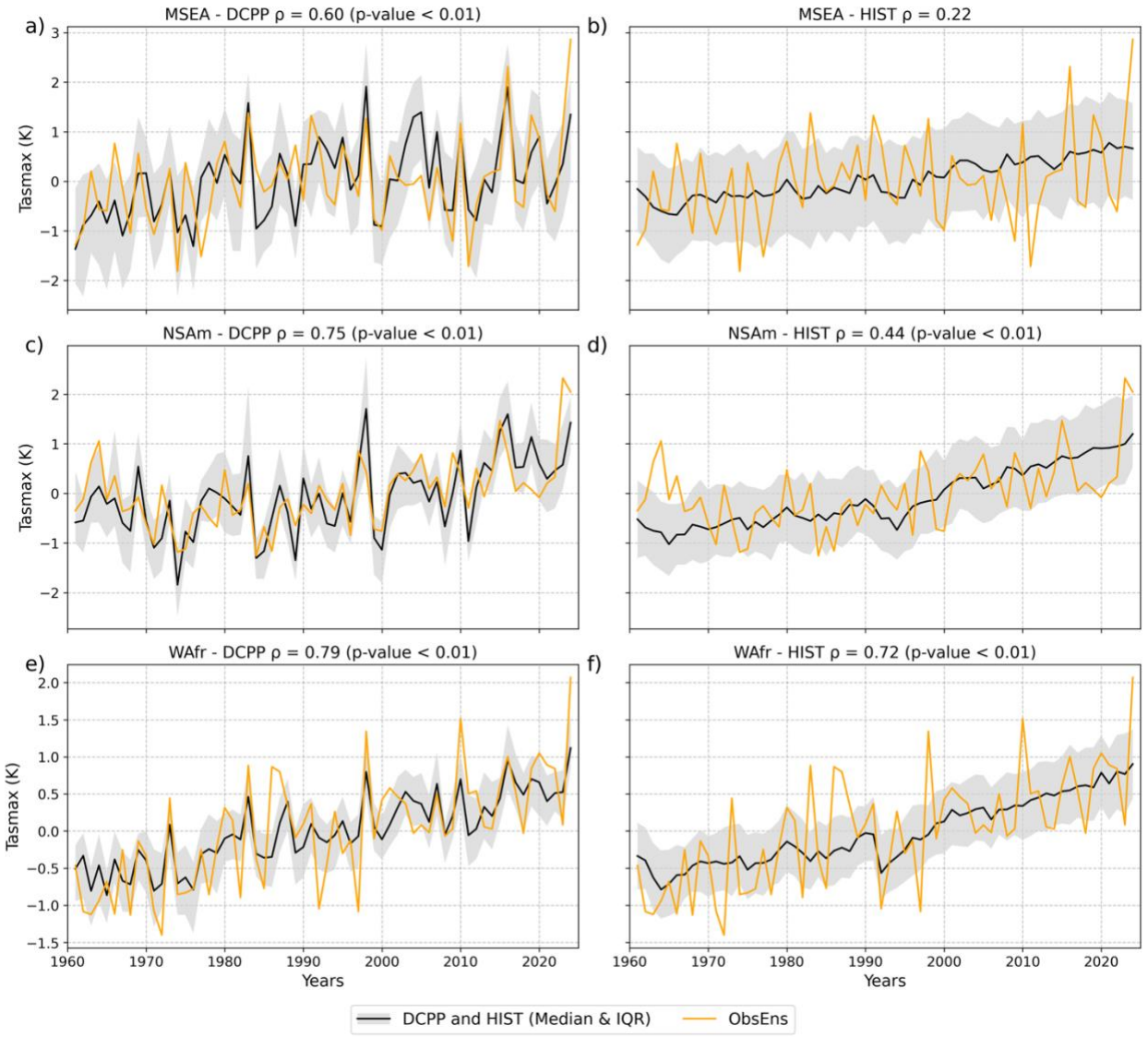


Figure S10. As Figure 3 but for tasmax 7-day averages computed as absolute values.

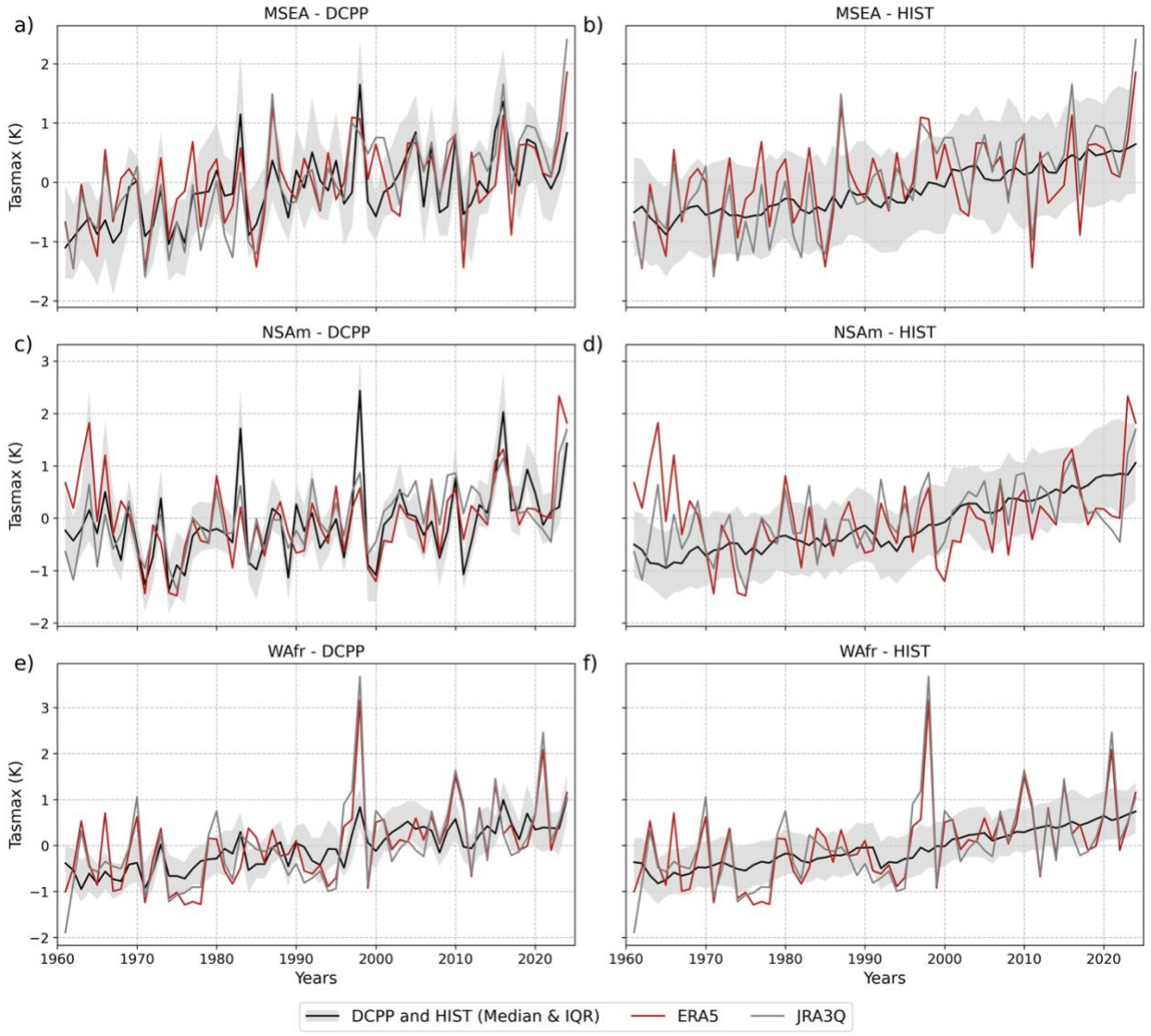


Figure S11. As Figure 3 but showing the individual observations-based datasets instead of ObsEns.

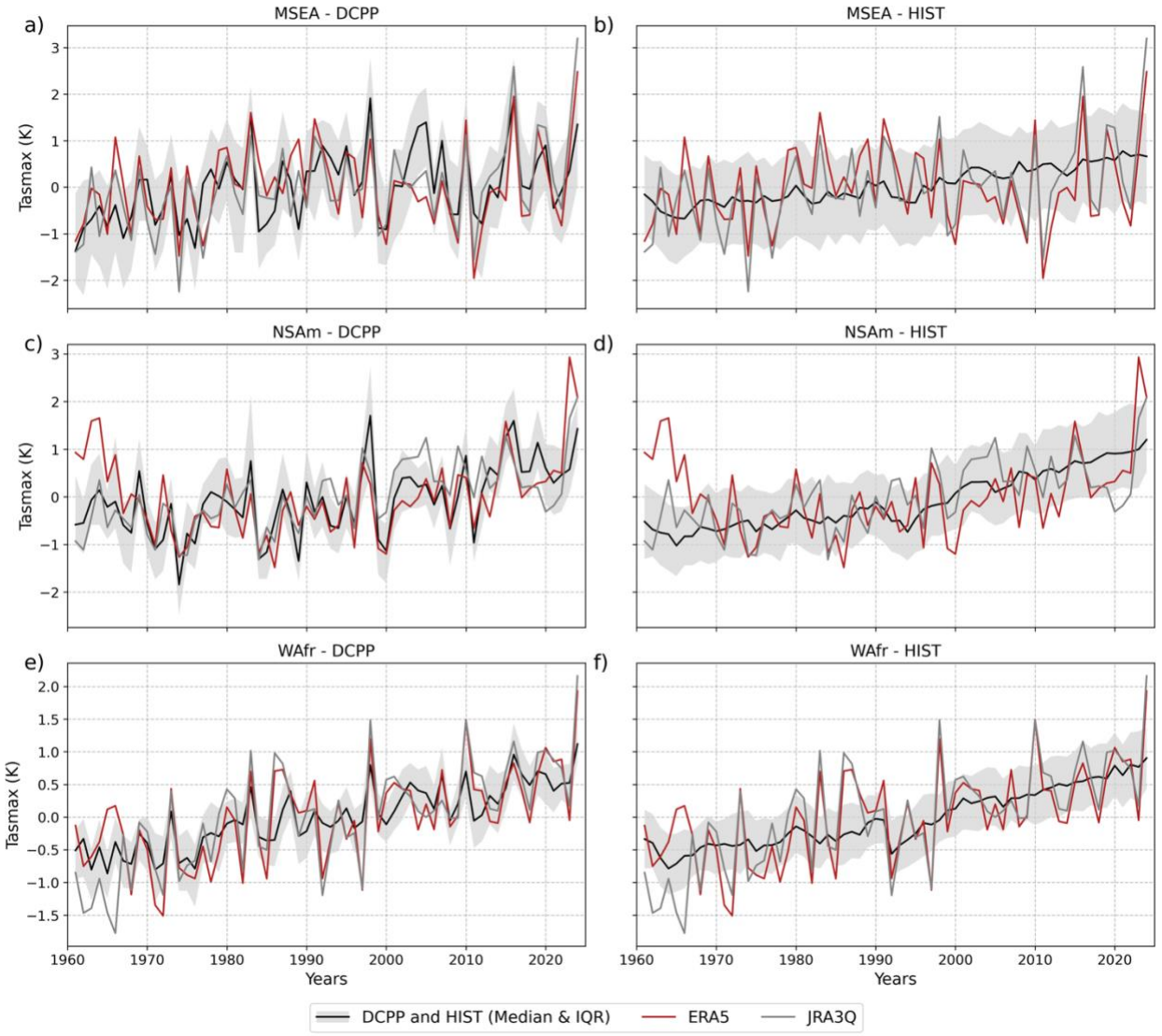


Figure S12. As Figure S8 but showing the individual observations-based datasets instead of ObsEns.

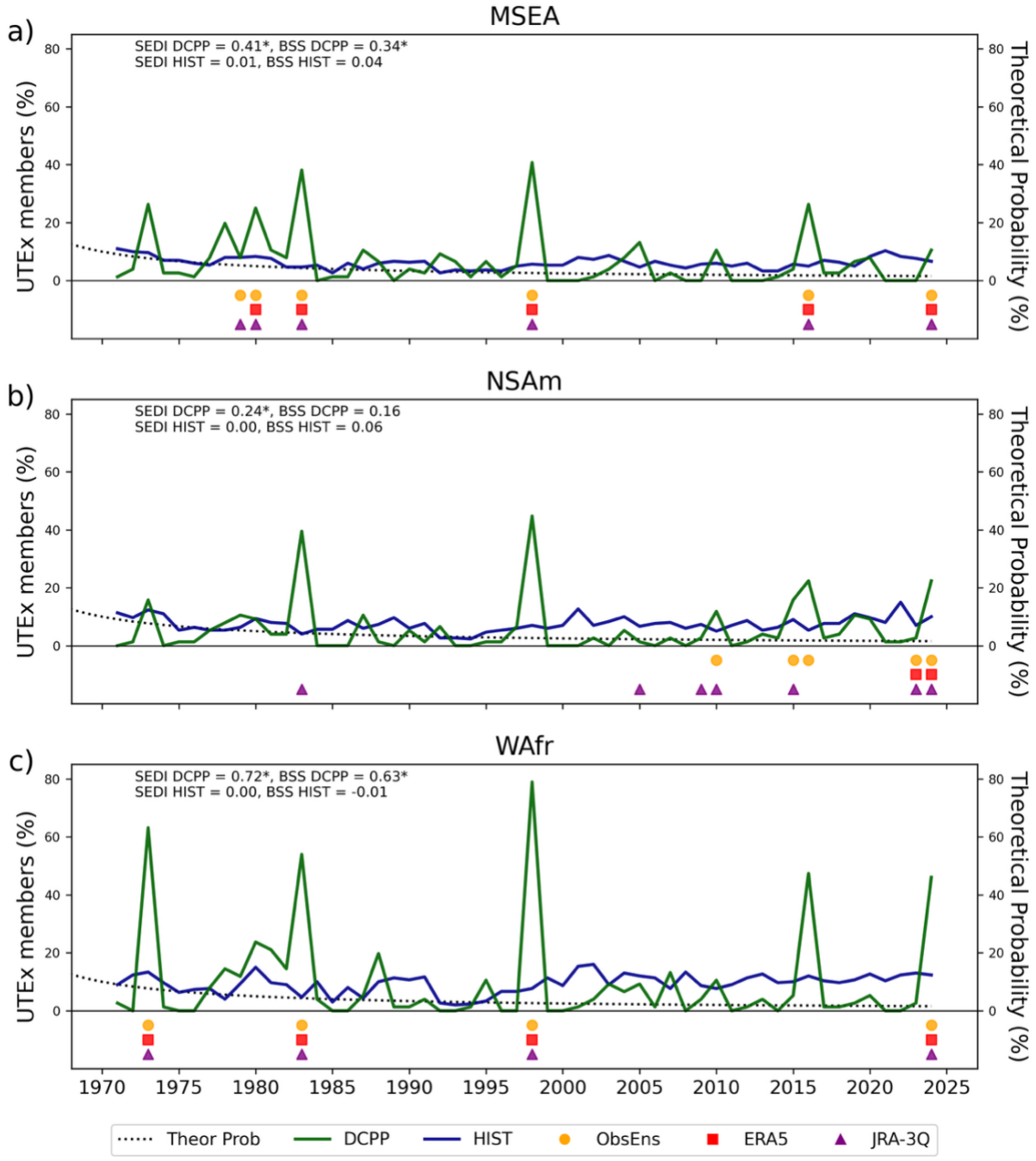


Figure S13. As Figure 4 but for UTEx computed based on absolute temperature values.

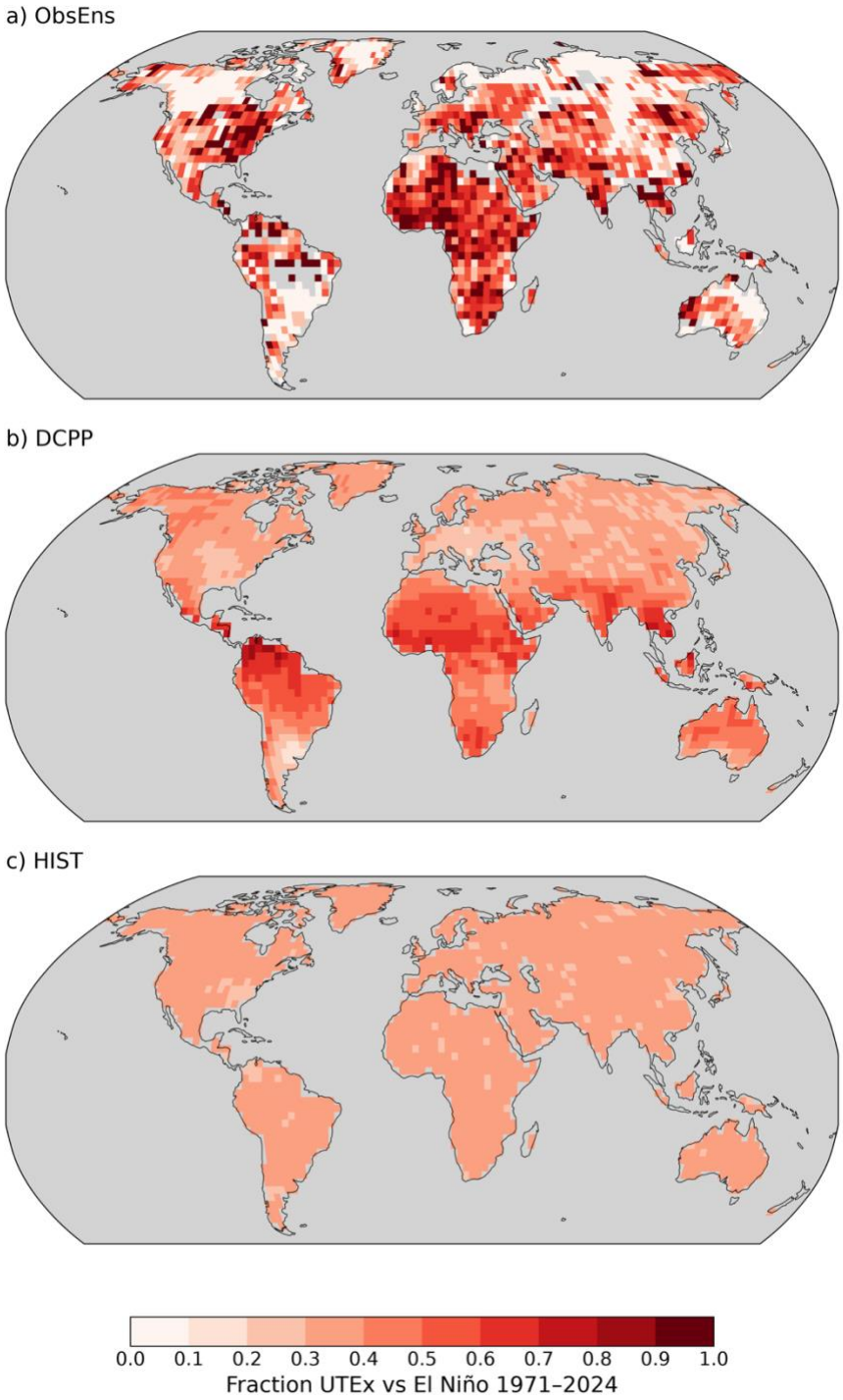


Figure S14. As Figure 5 but for UTEx computed based on absolute temperature values.

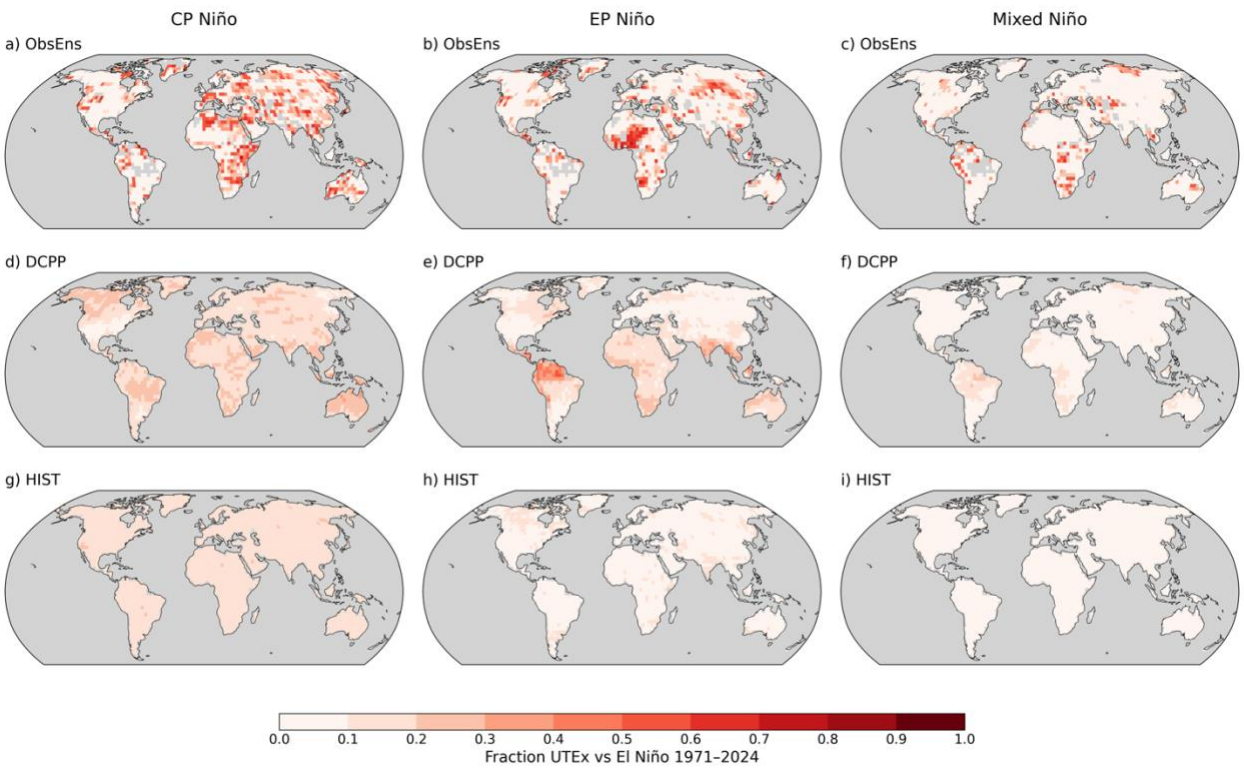


Figure S15. As Figure 5 but for (a,d,g) Central Pacific (CP) Niño, (b,e,h) Eastern Pacific (EP) Niño and (c,f,i) Mixed (Mix) Niño years, subsetted from the original 18 Niño years used in Figures 5 and S14. Note that 1980 fulfils our criteria of El Niño year but is not officially recognized as such because the SST anomalies were too weak and short-lived.

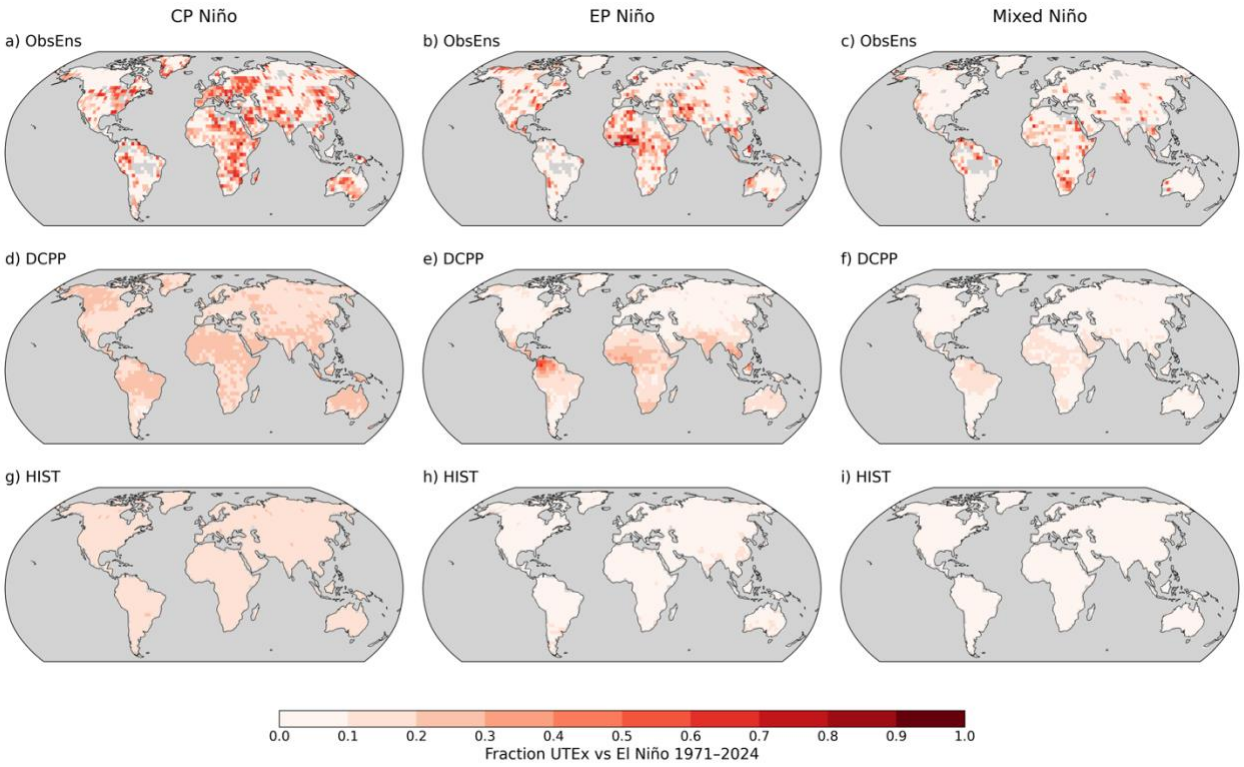


Figure S16. As Figure S14 but for (a,d,g) Central Pacific (CP) Niño, (b,e,h) Eastern Pacific (EP) Niño and (c,f,i) Mixed (Mix) Niño years, subsetted from the original 18 Niño years used in Figures 5 and S14. Note that 1980 fulfils our criteria of El Niño year but is not officially recognized as such because the SST anomalies were too weak and short-lived.

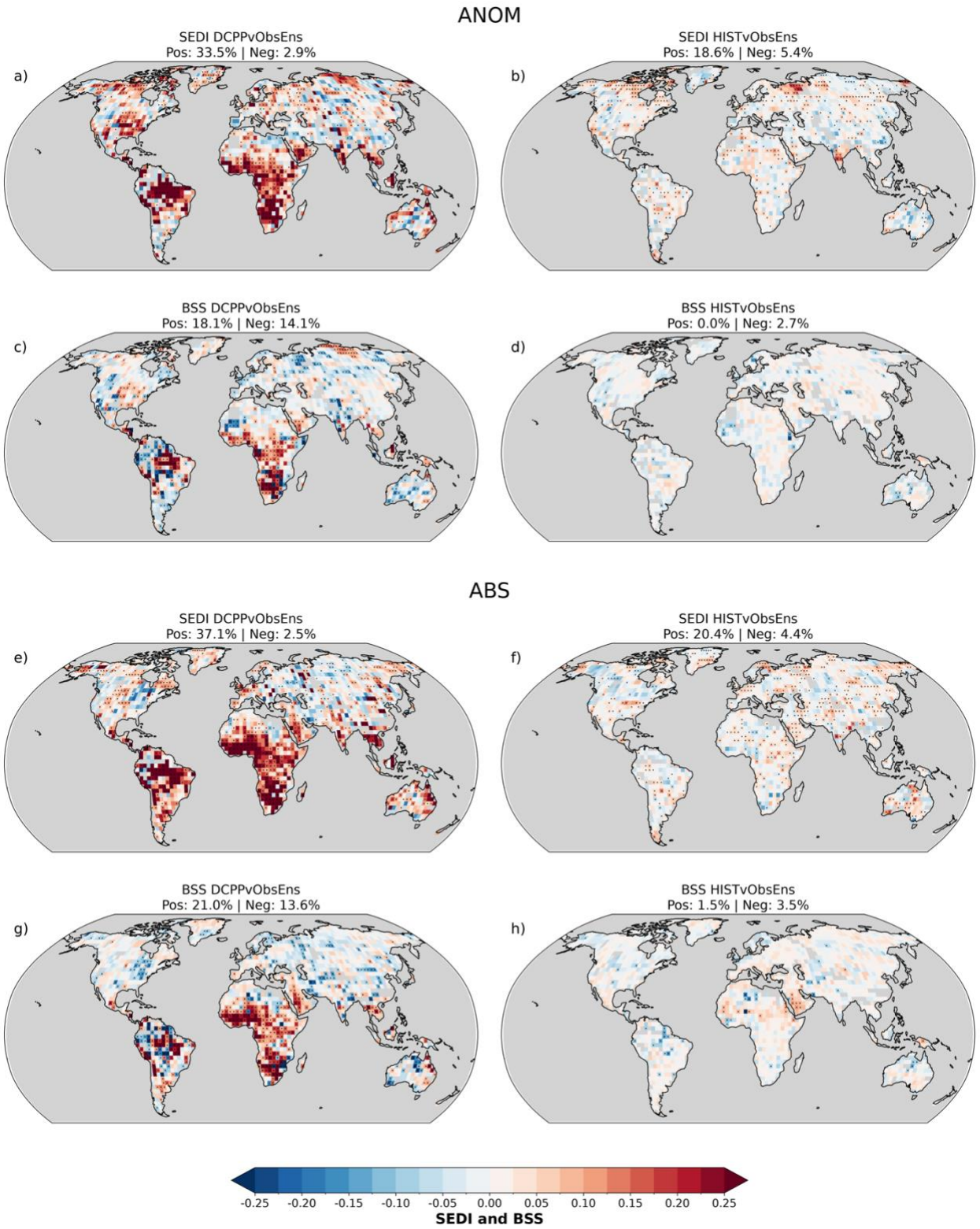


Figure S17. As Figures 1 and S3 but for UTEx and skill computed in the first six months of each calendar year (i.e. from January to June).

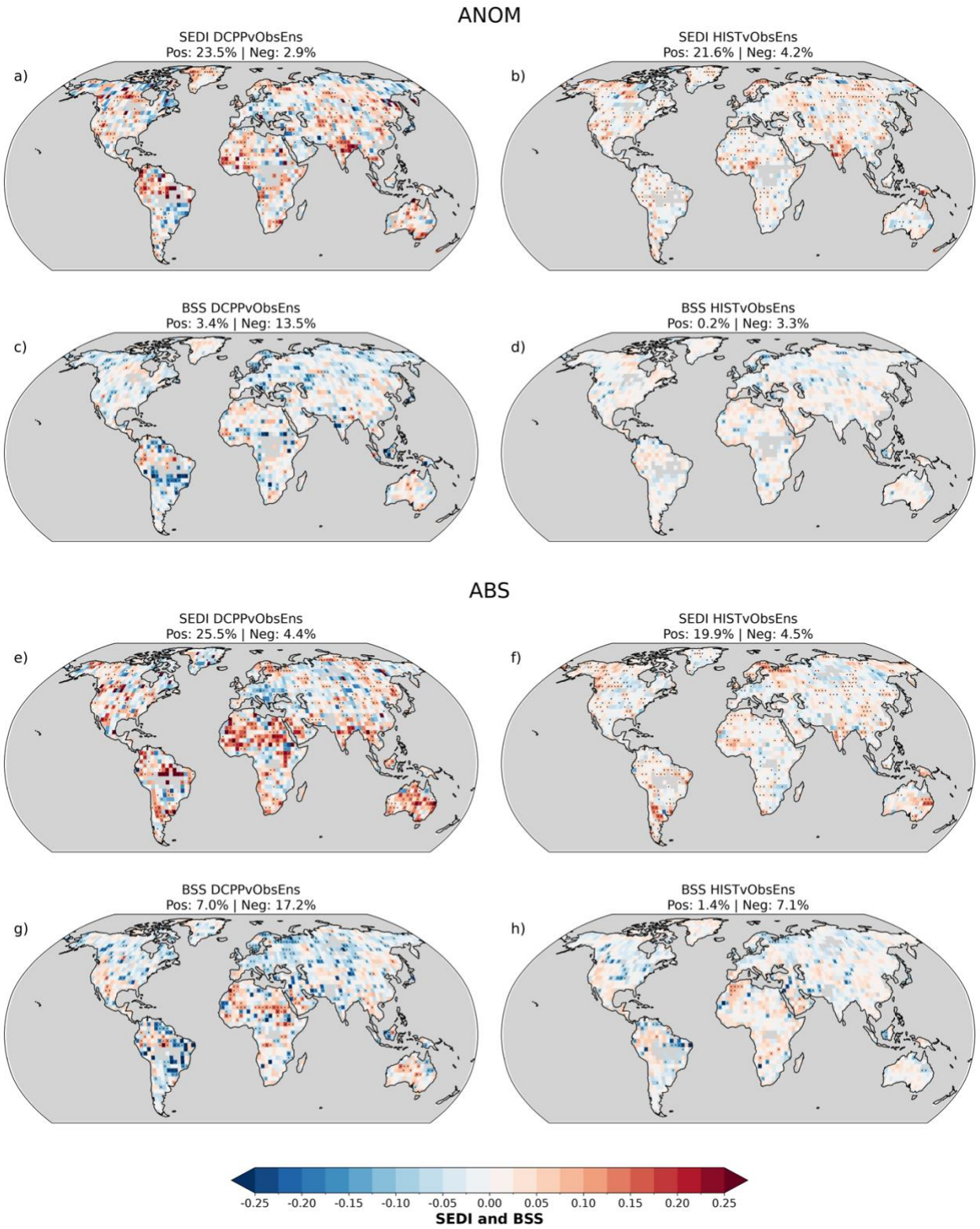


Figure S18. As Figures 1 and S3 but for UTEx and skill computed in the last six months of each calendar year (i.e. from July to December).

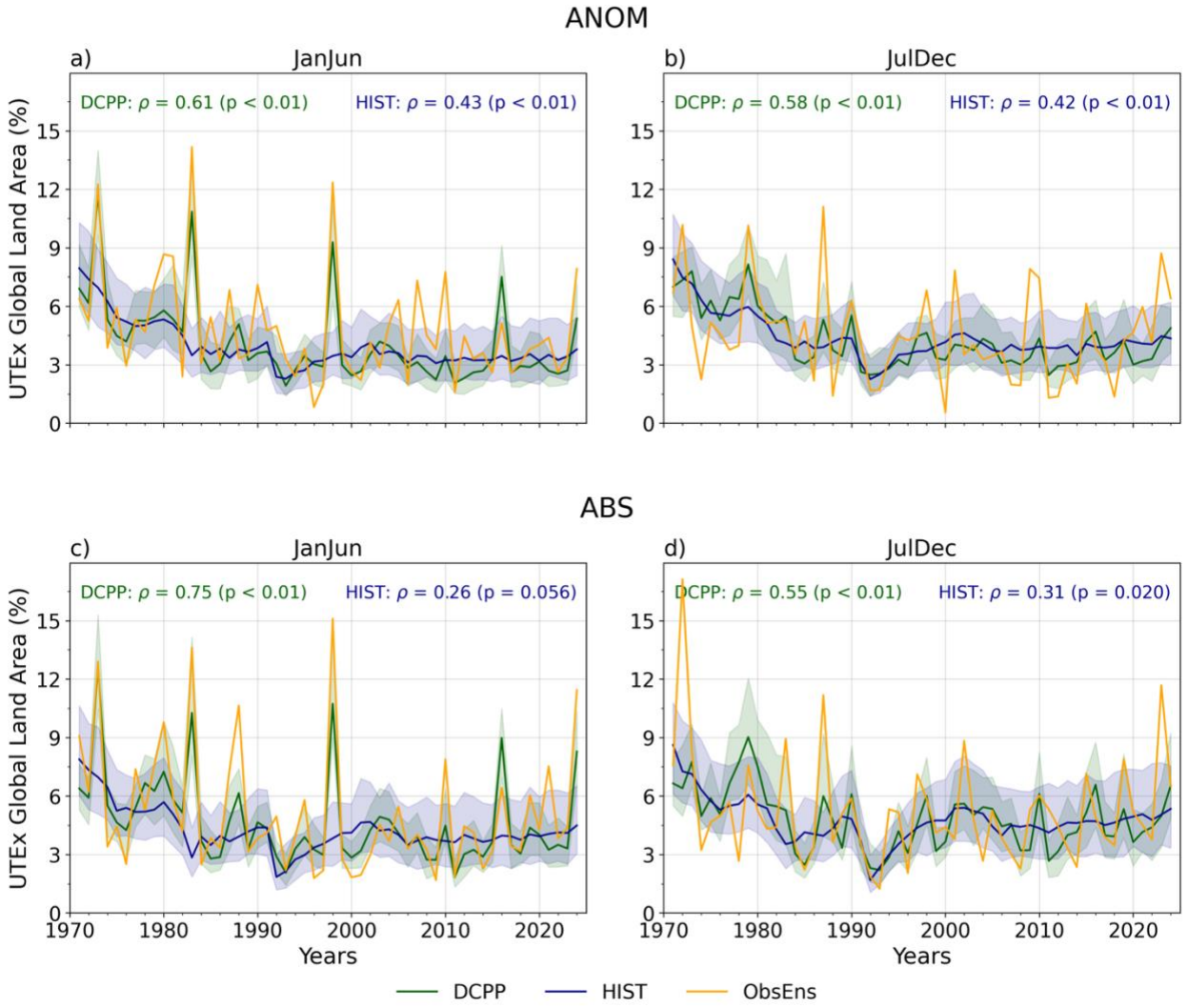


Figure S19. As Figures 2 (a-b) and S8 (c-d) but for UTEx Global Land Area (%) computed in the first (a, c) and last (b, d) six months of each calendar year (i.e. from January to June and from July to December).

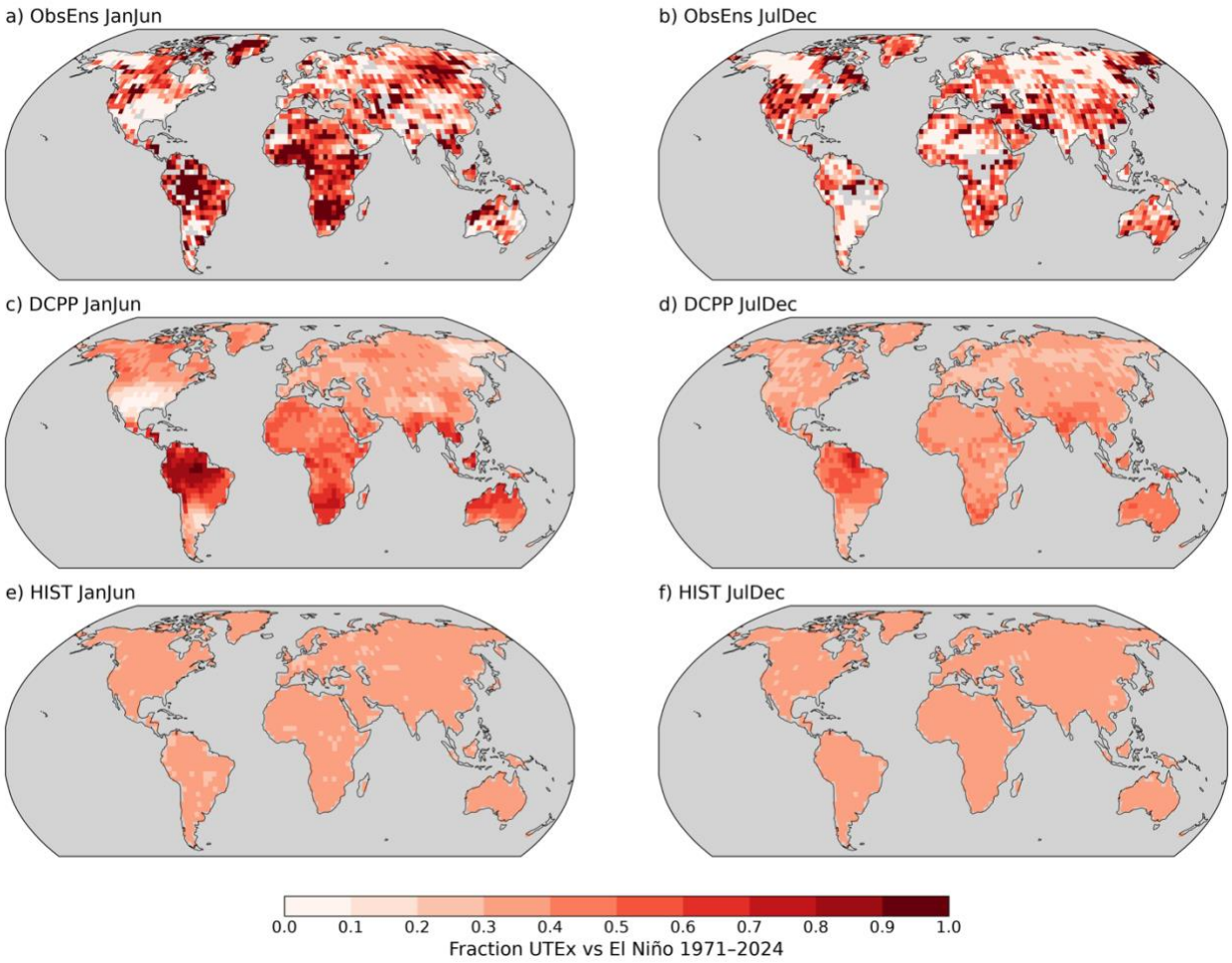


Figure S20. As Figure 5 but for UTEx computed in the first (a, c, e) and last (b, d, f) six months of each calendar year (i.e. from January to June and from July to December).

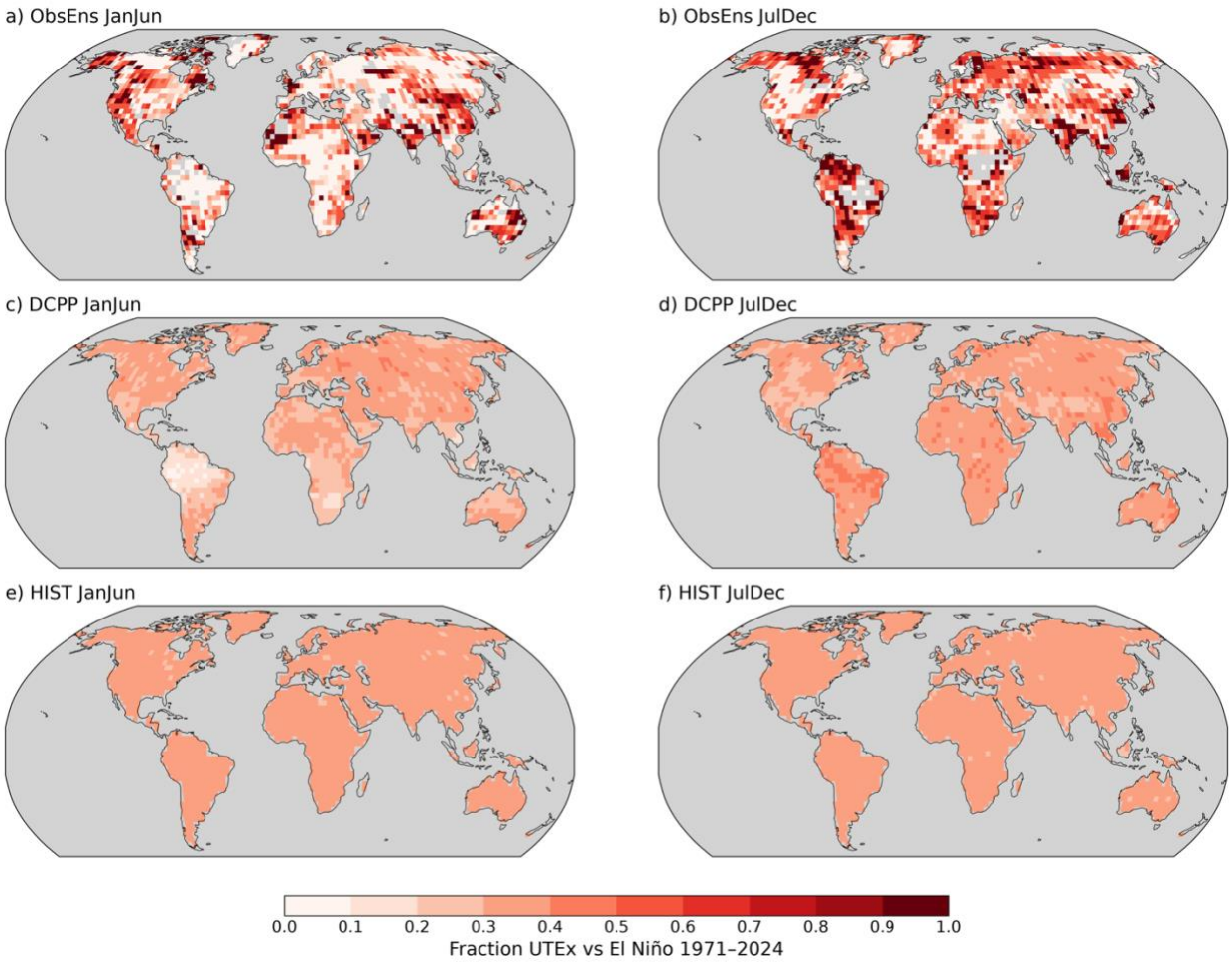


Figure S21. As Figure 5 but for UTEx computed over January-June and July-December half-year periods (1971-2024) and El Niño years identified as years ending with an El Niño month.

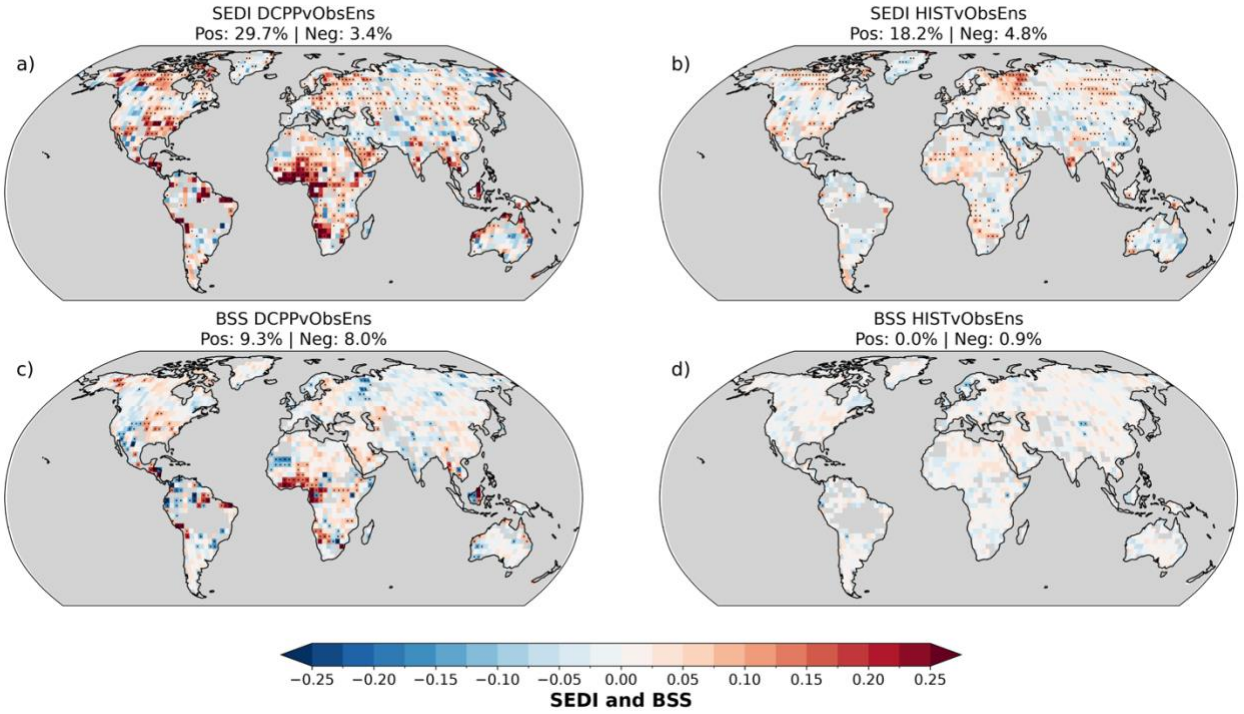


Figure S22. Same as Figure 1 but for two larger DCPP and HIST MMEs for the period 1971-2014. DCPP MME is composed of 158 hindcast members from 12 models and HIST MME from 525 Historical members from 45 models.

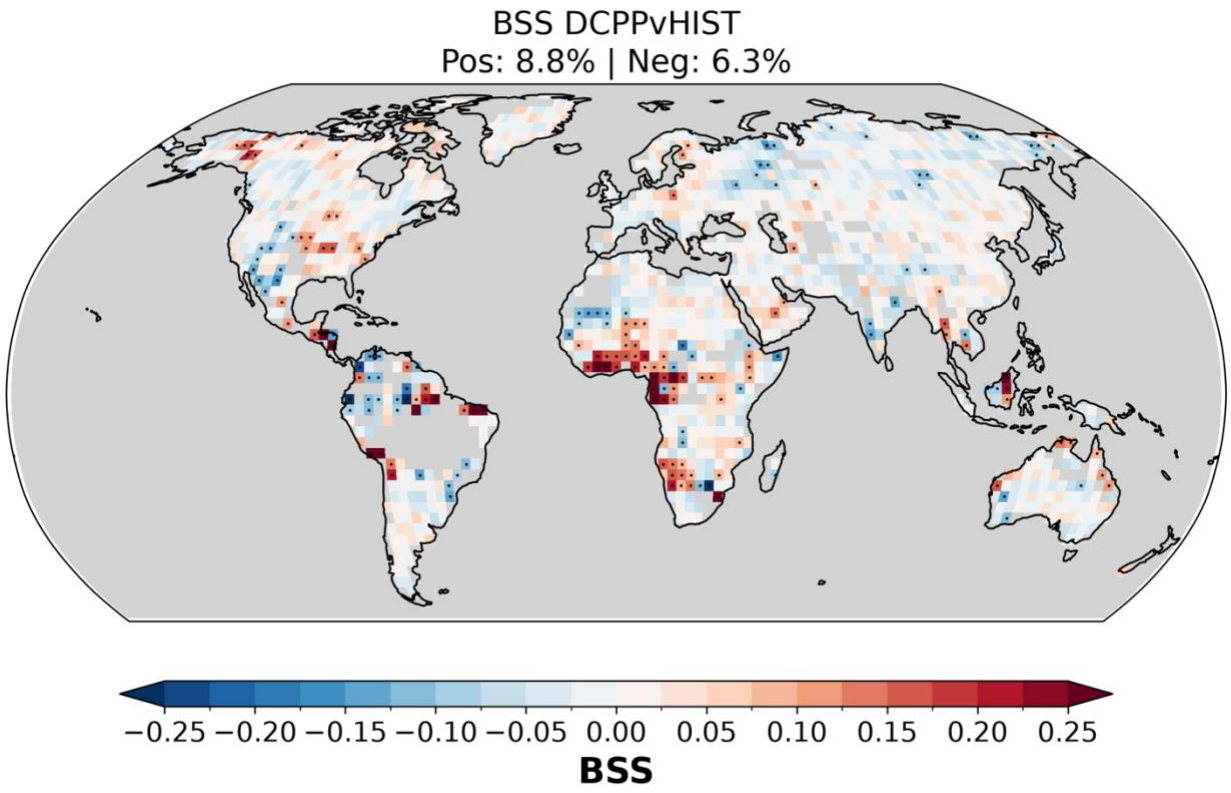


Figure S23. Same as Figure S2 but for the two larger DCPP and HIST MMEs for the period 1971-2014.

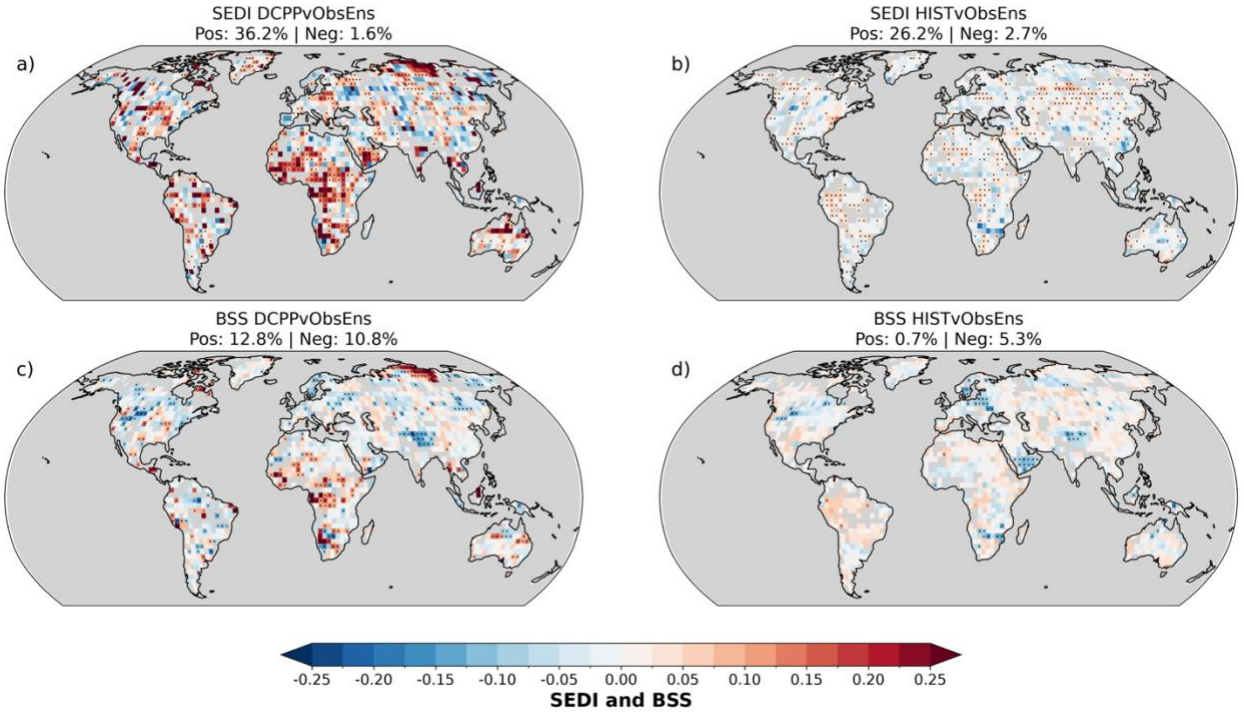


Figure S24. As Figure 1 but for UTEx and skill computed over the 1990-2024 period.

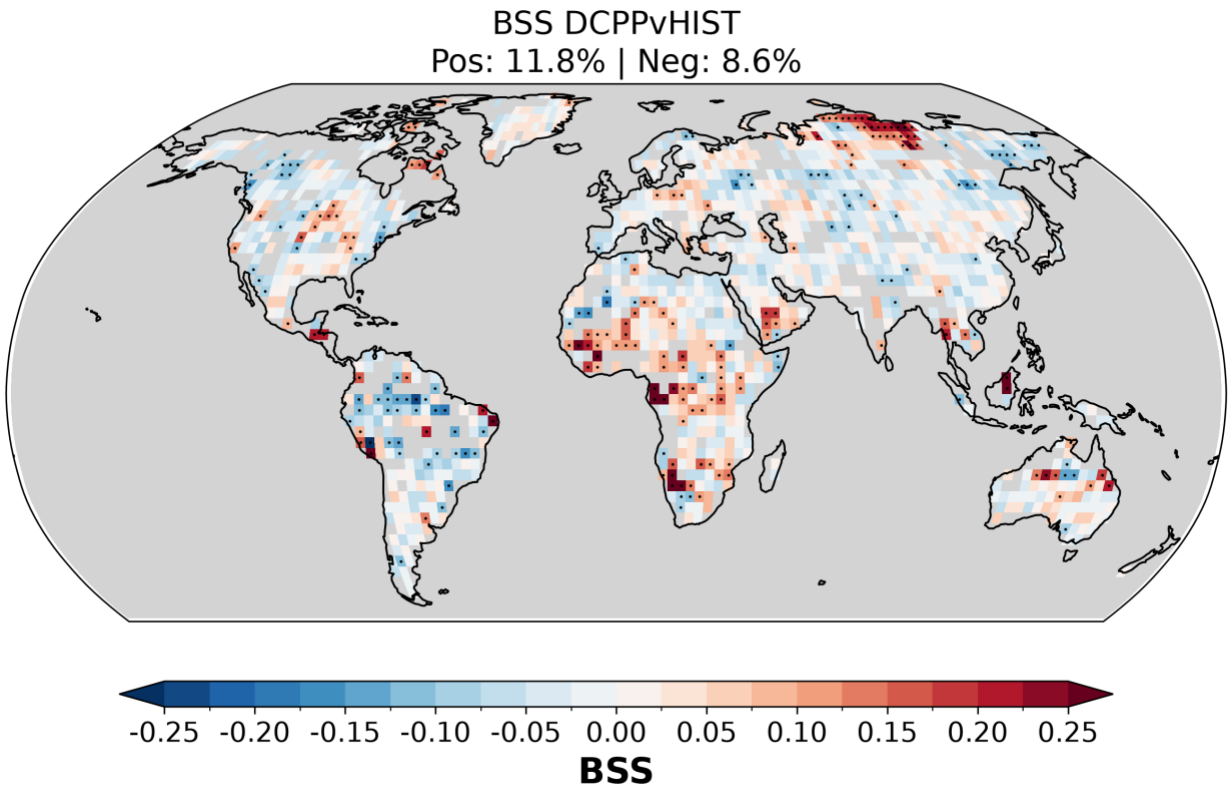


Figure S25. As Figure S2 but for UTEx and skill computed over the 1990-2024 period.

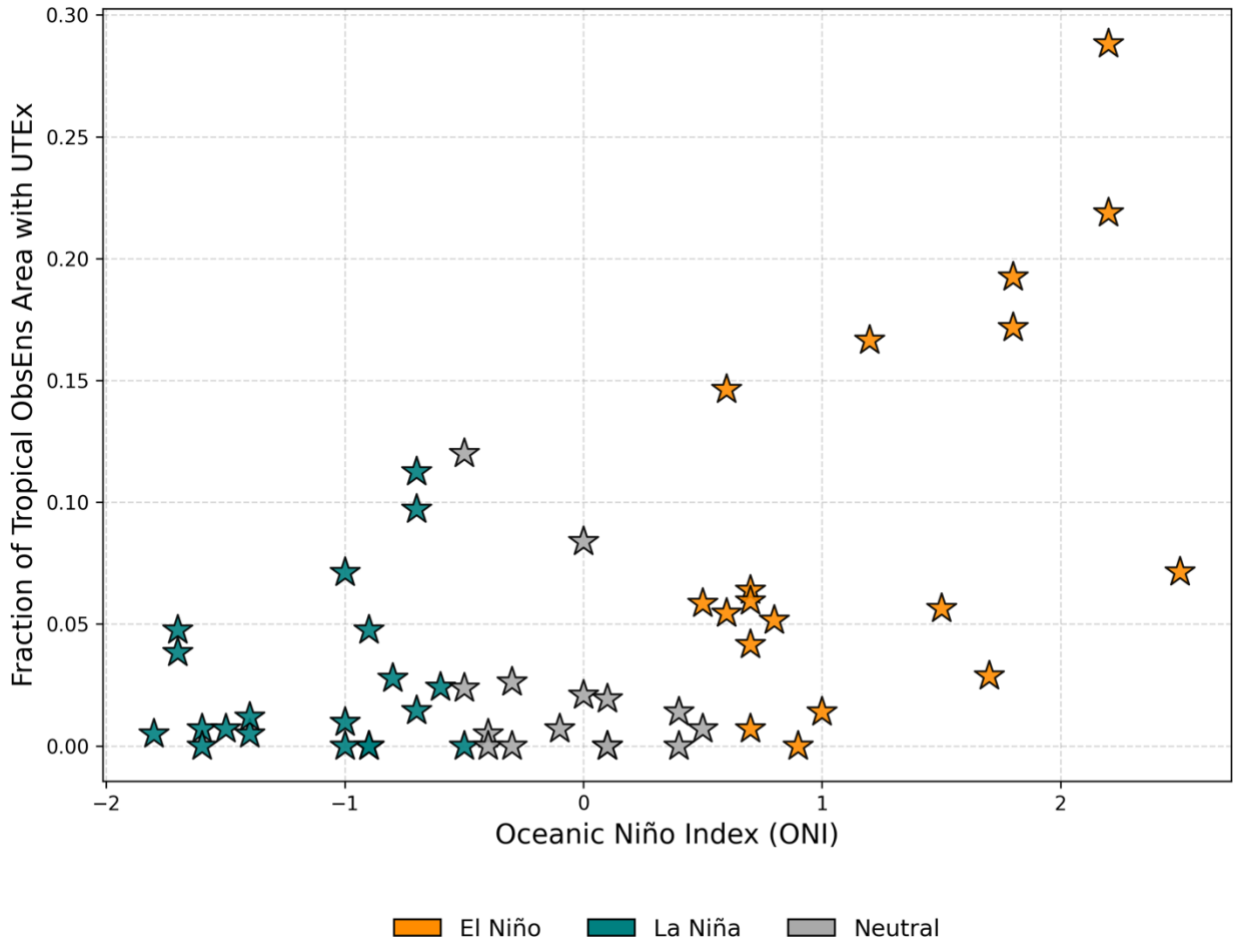


Figure S26. Fraction of tropical area impacted by UTEx as function of the ONI from 1971 to 2024. The fraction is shown for ObsEns overall field average of MSEA, NSAm and WAfr regions. Green, yellow and grey colors represent observed El Niño and La Niña years. UTEx are computed as anomalies and El Niño and La Niña years are obtained from the ONI as calendar years that start with an El Niño or La Niña month. ONI is computed from ERSST.v5[39] observational data over the Niño3.4 region (https://www.ncei.noaa.gov/access/monitoring/enso/sst) and the values shown represent the ones of the first month of the year.

Supporting Tables

Model	Institution	Members	# Members
CMCC-CM2-SR5	CMCC	r[1-10]i1p1f1	10
CanESM5	CCCma	r[1-20]i1p2f1	20
EC-Earth3	EC-Earth consortium	r[1-10]i4p1f1	10
HadGEM3-GC31-MM	MOHC	r[1-10]i1p1f2	10
MIROC6	MIROC	r[1-10]i1p1f1	10
MPI-ESM1-2-LR	MPI	r[1-16]i1p1f1	16

Table S1. List of 8 models and 76 members composing the CMIP6 DCPP ensemble. Data span the 1961-2024 period.

Model	Institution	Members	# Members
ACCESS-CM2	CSIRO - ARCCSS	r[1-5]i1p1f1	5
ACCESS-ESM1-5	CSIRO	r[1-40]i1p1f1	40
AWI-CM-1-1-MR	AWI	r1i1p1f1	1
AWI-ESM-1-REcoM	AWI	r1i1p1f1	1
BCC-CSM2-MR	BCC	r1i1p1f1	1
CanESM5	CCCma	r[1-20, 22-25]i1p1f1, r[1-12, 14-17, 20, 22-25]i1p2f1	45
CMCC-ESM2	CMCC	r1i1p1f1	1
CNRM-CM6-1	CNRM-CERFACS	r1i1p1f2	1
CNRM-ESM2-1	CNRM-CERFACS	r1i1p1f2	1
EC-Earth3-AerChem	EC-Earth consortium	r4i1p1f1	1
EC-Earth3-CC	EC-Earth consortium	r[1, 4, 6-13]i1p1f1	10
EC-Earth3-Veg-LR	EC-Earth consortium	r[1-3]i1p1f1	3
EC-Earth3-Veg	EC-Earth consortium	r[1-3, 5]i1p1f1	4
EC-Earth3	EC-Earth consortium	r[1-2, 4-7, 9-10, 12, 14, 16-25]i1p1f1	20
FGOALS-g3	CAS	r[1, 3-4]i1p1f1	3
GFDL-CM4	NOAA GFDL	r1i1p1f1	1
GFDL-ESM4	NOAA GFDL	r1i1p1f1	1
GISS-E2-1-G	NASA GISS	r1i1p1f2	1
HadGEM3-GC31-LL	MOHC	r[1-5]i1p1f3	5
INM-CM4-8	INM	r1i1p1f1	1
INM-CM5-0	INM	r1i1p1f1	1
IPSL-CM6A-LR	IPSL	r[1-6, 10-11, 14, 22, 25]i1p1f1	11
MIROC-ES2H	MIROC	r[1-3]i1p4f2	3
MIROC-ES2L	MIROC	r[1-30]i1p1f2	30
MIROC6	MIROC	r[1-50]i1p1f1	50
MPI-ESM1-2-HR	MPI	r[1-2]i1p1f1	2
MPI-ESM1-2-LR	MPI	r[1-30]i1p1f1	30
MRI-ESM2-0	MRI	r[1-5]i1p1f1	5
NESM3	NUIST	r[1-2]i1p1f1	2
NorESM2-LM	NorESM consortium	r[1-3]i1p1f1	3
NorESM2-MM	NorESM consortium	r[1-2]i1p1f1	2
TaiESM1	RCEC	r1i1p1f1	1
UKESM1-0-LL	MOHC	r[1-4, 8-12, 14, 16-19]i1p1f2	14

Table S2. As Table S1 but for the CMIP6 HIST ensemble of 33 models and 300 members.

Region	CMIP6 MME	Rean	ρ	p-value
MSEA	DCPP	ERA5	0.58	< 0.01
MSEA	DCPP	JRA3Q	0.69	< 0.01
MSEA	HIST	ERA5	0.36	< 0.01
MSEA	HIST	JRA3Q	0.60	< 0.01
NSAm	DCPP	ERA5	0.64	< 0.01
NSAm	DCPP	JRA3Q	0.71	< 0.01
NSAm	HIST	ERA5	0.21	< 0.10
NSAm	HIST	JRA3Q	0.49	< 0.01
WAfr	DCPP	ERA5	0.54	< 0.01
WAfr	DCPP	JRA3Q	0.54	< 0.01
WAfr	HIST	ERA5	0.53	< 0.01
WAfr	HIST	JRA3Q	0.51	< 0.01

Table S3. Regional Spearman's rank correlation coefficients (ρ) and corresponding p-values for near-surface maximum 7-day average temperatures (tasmax, K). These are computed between the CMIP6 DCPP, HIST MME medians and the two reanalysis datasets: ERA5 and JRA3Q. The three regions are Mainland Southeast Asia (MSEA), Northern South America (NSAm) and Western Africa (WAfr). The tasmax used in the correlations are computed as anomalies.

Region	CMIP6 MME	Rean	ρ	p-value
MSEA	DCPP	ERA5	0.54	< 0.01
MSEA	DCPP	JRA3Q	0.63	< 0.01
MSEA	HIST	ERA5	0.08	0.547
MSEA	HIST	JRA3Q	0.33	< 0.01
NSAm	DCPP	ERA5	0.62	< 0.01
NSAm	DCPP	JRA3Q	0.73	< 0.01
NSAm	HIST	ERA5	0.25	< 0.10
NSAm	HIST	JRA3Q	0.58	< 0.01
WAfr	DCPP	ERA5	0.72	< 0.01
WAfr	DCPP	JRA3Q	0.79	< 0.01
WAfr	HIST	ERA5	0.62	< 0.01
WAfr	HIST	JRA3Q	0.72	< 0.01

Table S4. Same as Table S3 but for tasmax computed as absolute values.

	BSS DCPPvHIST ObsEns	
	Anom	Abs
MSEA	**0.22**	**0.32**
NSAm	0.09	0.11
WAfr	**0.37**	**0.64**

Table S5. Regional BSS added value of DCPP against HIST for the three regions (MSEA, NSAm and WAfr) with UTEx computed as anomalies and absolute values with ObsEns as reference dataset for 1961-2024. Values in bold are statistically significant (p-value <0.05).

Mainland Southeast Asia (MSEA)				
	1961-2024			
	SEDI		BSS	
	Anom	Abs	Anom	Abs
DCPPvERA5	**0.35**	**0.41**	0.13	**0.40**
HISTvERA5	-0.03	0.01	-0.03	0.03
DCPPvHIST ERA5	-	-	0.15	**0.38**
DCPPvJRA3Q	**0.35**	**0.45**	**0.25**	**0.34**
HISTvJRA3Q	-0.04	0.00	0.02	0.04
DCPPvHIST JRA3Q	-	-	**0.24**	**0.32**

Table S6. Regional annual prediction skill for MSEA computed for the 1961-2024 MME. DCPPvHIST represent the BSS of DCPP using HIST as reference forecast and ERA5 and JRA3Q as observational datasets, indicating the added skill of DCPP over HIST. Values in bold are statistically significant (p-value <0.05).

Northern South America (NSAm)				
	1961-2024			
	SEDI		BSS	
	Anom	Abs	Anom	Abs
DCPPvERA5	0.15	0.15	-0.03	-0.03
HISTvERA5	0.03	0.03	0.03	0.01
DCPPvHIST ERA5	-	-	-0.06	-0.04
DCPPvJRA3Q	**0.35**	**0.22**	**0.24**	0.15
HISTvJRA3Q	0.00	0.00	0.03	0.06
DCPPvHIST JRA3Q	-	-	**0.22**	0.10

Table S7. As Table S6 but for NSAm.

Western Africa (WAfr)				
	1961-2024			
	SEDI		BSS	
	Anom	Abs	Anom	Abs
DCPPvERA5	**0.78**	**0.72**	**0.33**	**0.63**
HISTvERA5	0.02	0.00	-0.07	-0.01
DCPPvHIST ERA5	-	-	**0.37**	**0.64**
DCPPvJRA3Q	**0.58**	**0.72**	**0.45**	**0.63**
HISTvJRA3Q	0.01	0.00	0.01	-0.01
DCPPvHIST JRA3Q	-	-	**0.44**	**0.64**

Table S8. As Table S6 but for WAfr.

Peak Year	ENSO Cycle	Classification	Reference
1973	1972–73	Eastern Pacific (EP)	Kao & Yu, 2009
1977	1976–77	Eastern Pacific (EP)	Kao & Yu, 2009
1978	1977–78	Central Pacific (CP)	Kao & Yu, 2009
1980	-	-	-
1983	1982–83	Eastern Pacific (EP)	Kao & Yu, 2009
1987	1986–87	Central Pacific (CP)	Kao & Yu, 2009
1988	1987–88	Central Pacific (CP)	Kao & Yu, 2009
1992	1991–92	Central Pacific (CP)	Kao & Yu, 2009
1995	1994–95	Central Pacific (CP)	Kao & Yu, 2009
1998	1997–98	Eastern Pacific (EP)	Kao & Yu, 2009
2003	2002–03	Central Pacific (CP)	Kao & Yu, 2009
2005	2004–05	Central Pacific (CP)	Kao & Yu, 2009
2007	2006–07	Central Pacific (CP)	Kao & Yu, 2009
2010	2009–10	Central Pacific (CP)	Racault et al., 2017
2015	2014-15	Mixed	Santoso et al., 2017
2016	2015–16	Mixed	Santoso et al., 2017
2019	2018–19	Central Pacific (CP)	Liu et al., 2020
2024	2023–24	Mixed	Geng et al., 2024

Table S9. List of the 18 El Niño years computed in Figures 5 and S14, divided into Central Pacific (CP), Eastern Pacific (EP) and Mixed El Niño years. Note that 1980 fulfils our criteria of El Niño years but is not officially recognized as such because the SST anomalies were too weak and short-lived.